

Climate change threatens archeologically significant ice patches: insights into their age, internal structure, mass balance and climate sensitivity

Rune Strand Ødegård¹, Atle Nesje², Ketil Isaksen³,
Liss Marie Andreassen⁴, Trond Eiken⁵, Margit Schwikowski⁶
and Chiara Uglietti⁶

[1]{Norwegian University of Science and Technology, Gjøvik, Norway}

[2]{University of Bergen, Bergen, Norway}

[3]{Norwegian Meteorological Institute, Oslo, Norway}

[4]{Norwegian Water Resources and Energy Directorate, Oslo, Norway}

[5]{Department of Geosciences, University of Oslo, Oslo, Norway}

[6]{Paul Scherrer Institute, Villigen, Switzerland}

Correspondence to: R.S. Ødegård (rune.oedegaard@ntnu.no)

Abstract

Despite numerous spectacular archaeological discoveries worldwide related to melting ice patches and the emerging field of glacial archaeology, governing processes related to ice patch development during Holocene and their sensitivity to climate change are still largely unexplored. Here we present new results from an extensive 6-year (2009-2015) field experiment at Juvfonne ice patch in Jotunheimen in central southern Norway. Our results show that the ice patch existed continuously since the late Mesolithic period. Organic-rich layers and carbonaceous aerosols embedded in clear ice shows ages spanning from modern at the surface to ca. 7600 cal. years BP at the bottom. This is the oldest dating of ice in mainland Norway. The expanding ice patch covered moss mats appearing along the margin of Juvfonne in 2014 about 2000 years ago. During the study period, the mass balance record shows a strong negative balance, and the annual balance is highly asymmetric over short distances. Snow accumulation is poorly correlated with estimated winter precipitation and single storm

events may contribute significantly to the total winter balance. Snow accumulation is approx. 20 % higher in the frontal area compared to the upper central part of the ice patch. There is sufficient melt water to bring the permeable snowpack to an isothermal state within a few weeks in early summer. Below the seasonal snowpack, ice temperatures are between -2 and -4°C. Juvfonne has clear ice stratification of isochronic origin. The cumulative deformation of ice over millennia could explain the observed curved layering in the basal parts of the ice patch, which makes it difficult to relate the present thickness to previous thickness of the ice patch. Ice deformation and surface processes (i.e. wind and melt water) may have caused significant displacement of artefacts from their original position. Thus, the dating and position of artefacts cannot be used directly to reconstruct previous ice patch extent. In the perspective of surface energy and mass balance, ice patches are in the transition zone between permafrost terrain and glaciers. Future research will need to carefully address this interaction to build reliable models.

1 Introduction

The emergence of glacial archaeology is described by Andrews and Mackay (2012) and Dixon et al. (2014). In archaeology, the term ‘glacial archaeology’ or ‘snow patch archaeology’ refers to several alpine contexts in different regions of the world (Callanan, 2010). The release of Ötzi’s 5300 year old body from the ice in northern Italy marked the beginning of a number of remarkable archaeological discoveries world-wide connected to melting ice and thawing permafrost in the high mountains (Spindler, 1994). Discoveries are known from the Alps (Grosjean et al., 2007; Suter et al., 2005), mummies in Greenland (Hansen et al., 1985) and the Andes Mountains (Ceruti, 2004), and from archaeological finds at retreating ice patches in North America (Brunswig, 2014; Dixon et al., 2005; Farnell et al., 2004; Hare et al., 2012; Lee, 2012; Meulendyk et al., 2012). When analysing the number of artefacts on a global scale during the Holocene, there is a negative correlation between periods of glacial advance and the number of artefacts. This is particularly the case in the Alps and North America (Reckin, 2013), but a similar pattern is also found in Norway (Nesje et al., 2012). The question is if this is caused by changes in climate dependent preservation conditions or decreased human use of these areas in periods of cold climate.

In Norway, there has been an increasing focus on ice patches since the extreme melting in southern Norway in the autumn of 2006. There are about 3000 known artefact finds globally

1 from ice patches. Most of these have melted out during the last three decades. Approximately
2 2000 of these archaeological finds are in central southern Norway, making it by far the most
3 find-rich region in the world (Curry, 2014, pers.comm. Lars Pilø). Among the most
4 spectacular finds is a Bronze Age leather shoe that melted out in late autumn 2006 and a well-
5 preserved tunic dated between 230-390 (Common Era) CE (Finstad and Vedeler, 2008;
6 Vedeler and Jørgensen, 2013). The shoe was dated to be around 3400 years old (1429-1257
7 Before Common Era (BCE)), and is by far the oldest shoe found in Norway. Dates are given
8 in calibrated ages (BCE/CE) including 1 sigma errors (σ) when referencing archaeological
9 finds in Norway. Radiocarbon dates from ice patches are referenced as calibrated years
10 Before Present (BP=1950CE).

11 The geoscience of old ice patches is still in its infancy and the geoscience literature about ice
12 patches is sparse compared to glacial archaeology. Within the glaciological community it is
13 commonly differentiated between glaciers and snowfields and active or inactive ice
14 (UNESCO, 1970). Snowfields may be seasonal or perennial. Seasonal snowfields melt during
15 the summer. Perennial snowfields exist for two years or more. Smaller ice bodies without
16 significant movement may be remnants of a past active glacier or a perennial snowfield and
17 are commonly referred to as glacierets. In this paper, we use ice patch for perennial
18 snowfields and glacierets. Ice patches are, in contrast to glaciers, mostly stagnant and
19 therefore, do not convey mass from an accumulation towards an ablation area. In fact, ice
20 patches often do not exhibit distinct glacier facies such as a firn area. In the wet-snow zone,
21 the transformation of snow to ice is fast by metamorphism and refreezing of melt water.
22 (Kawasaki et al., 1993). Ice patches and surrounding terrain are generally underlain by
23 permafrost (Haeberli et al., 2004). There are few studies related to the thermal regime, mass
24 balance and dynamics (Eveland et al., 2013; Fukui, 2003; Fukui and Iida, 2011; Sato et al.,
25 1984). Fujita et al. (2010) concluded that they exist below the altitude of the regional
26 equilibrium-line altitude (ELA) of glaciers. A study by Glazirin et al. (2004) showed that they
27 can modify the nearby wind field. The mentioned studies have documented feedbacks
28 between ice patch size and both summer ablation and winter snow accumulation. The spatial
29 variability of the turbulent fluxes in an alpine terrain is of particular interest to ice patches. Ice
30 patches are influenced by advective heat transfer in summer (Essery et al., 2006; Mott et al.,
31 2015; Pohl et al., 2006). The sensible heat flux is reported to be to twice the net radiation
32 input for melting snow (Morris, 1989).

1 Despite some progress in these studies, the state of knowledge is not at a level to design
2 reliable models of how ice patches have developed during the Holocene and to evaluate their
3 sensitivity to future climate changes. The main objective of this study is to help fill this
4 knowledge gap based on a 6-year field experiment at Juvfonne ice patch (Fig. 1 and 2),
5 located in Jotunheimen in central southern Norway.

6 The overall objective of this study is to do an exploratory data analysis of field data to better
7 understand the governing processes of ice patch mass balance and Holocene development.
8 The long-term objective is to design reliable models of the growth and decline of ice patches
9 in this alpine environment. One additional dimension in this research is the cooperation with
10 the archaeologist to help them in their interpretation of finds and give advice regarding future
11 development. A multi-disciplinary approach was chosen, combining a set of new geophysical
12 data, radiocarbon dating, mass balance measurements and visual observations from two 30-70
13 m tunnels that were excavated into the central parts of the ice patch to better understand (1)
14 the age, (2) the mass balance, (3) the thermal regime, (4) ice layering and deformation on
15 Holocene time scale and finally (5) the physical processes relevant to artefact displacement
16 and preservation.

18 **2 Field site and physical setting**

19 In central southern Norway the archaeologists have so far identified more than 65 sites with
20 finds related to ice patches, but many sites with potential finds have not been checked in the
21 field. The archaeological finds are related to reindeer hunting. The snowfields are an
22 important refuge for the reindeers during hot summer days, giving them relief from pestering
23 insects. The focus of this study is the ice patch Juvfonne (61.676°N, 8.354°E) and the
24 surrounding terrain (Fig. 1 and 2). This site is a well-preserved Iron Age hunting 'station'
25 documented by more than 600 registered wooden artefacts and 50 hunting blinds.
26 Radiocarbon dating of artefacts shows ages in two separate time intervals, 246-534 CE and
27 804-898 CE (Nesje et al., 2012). The geoscience studies at Juvfonne started in 2009 (Ødegård
28 et al., 2011). Nesje et al. (2012) gave a comprehensive presentation and discussion of
29 archaeological finds in central southern Norway related to Late Holocene climate history.

30 The width of the ice patch is approx. 500 m and upslope length 350 m. Juvfonne had an area
31 of 0.15 km² and ranged in altitude from 1839 to 1993 m a.s.l. in 2010 (Andreassen, 2011).
32 The mean surface slope is 17 degrees and the ice patch has a north easterly aspect.

1 Due to snowdrift by prevailing westerly winds during the accumulation season, Juvfonne is
2 below the regional temperature-precipitation equilibrium-line altitude (TP-ELA). Annual
3 surface mass balance measurements have been conducted on three glaciers (since 1949 at
4 Storbreen and 1962 at Hellstugubreen and Gråsubreen) in the Jotunheimen mountain region
5 (Andreassen et al., 2005; Andreassen and Winsvold, 2012). The ELA increases with distance
6 from coast from 1780 m a.s.l. at Storbreen to 2150 m a.s.l. at Gråsubreen (Kjøllmoen et al.,
7 2011). Except for a transient mass surplus from 1989-1995 due to increased winter
8 precipitation in this period, the glaciers have lost mass. Map surveys and inventory data show
9 a reduction in area of the glaciers in Jotunheimen of about 10 % from the 1960s to 2003
10 (Andreassen et al., 2008).

11 Juvfonne is well within the mountain permafrost zone. Present permafrost thicknesses at
12 elevations where we find perennial ice patches (\sim 1700 m a.s.l.) can be estimated to be more
13 than 100 m. Observations of ground thermal regimes (Farbrot et al., 2011; Harris et al., 2009),
14 bottom temperature of snow cover (BTS) (Farbrot et al., 2011; Isaksen et al., 2002; Ødegård,
15 1993) and geophysical surveys to delineate the altitudinal limit of the permafrost (Hauck et
16 al., 2004; Isaksen et al., 2011) along with spatial numerical equilibrium and transient
17 permafrost models (Gisnås et al., 2013; Gisnås et al., 2015; Hipp et al., 2012; Westermann et
18 al., 2013) indicate a lower limit of permafrost at 1450-1600 m a.s.l. in the area.

19 Juvfonne is at a distance of 750 m and at the same altitude as the permafrost boreholes (the
20 P30 and 31 Permafrost and Climate in Europe (PACE) boreholes) and climate monitoring site
21 at Juvvasshøe (Sollid et al., 2000)(see Fig. 2). The site has a record of ground temperatures
22 and meteorological observations since September 1999. Mean annual air temperature for the
23 period 2000-2015 is -3.5 °C. At 15 m depth, the permafrost temperature ranges from a
24 minimum of -3.1 °C in 1999 to a maximum of -2.5 °C recorded in 2008. The active layer
25 thickness has varied between 2.0 and 2.4 m and permafrost thickness is estimated to exceed
26 300 m (Isaksen et al., 2011). In 2008, an altitudinal transect of boreholes and adjacent air
27 temperature sensors were installed at three sites ranging from shallow seasonal frost to
28 permafrost (Farbrot et al 2013).

29 For the period 1961-1990, the mean annual precipitation is estimated to be between 800mm
30 a^{-1} and 1000mm a^{-1} at 1900 m a.s.l. at Juvfonne (Norwegian Meteorological Institute,
31 unpublished data).

Results of analysis from sediment cores in the nearby Juvvatnet was used to reconstruct the glacier activity of Kjelebrea and Vesljuvbrea (Nesje et al., 2012) following the methodology described by Bakke et al. (2010). The results indicate that the late Holocene variations of these glaciers are largely in agreement with size variations of other glaciers in the Jotunheimen area (Matthews and Dresser, 2008; Nesje, 2009). Lichenometry suggests that the margin of Juvfonne extended ~250 m from its present position during the ‘Little Ice Age’(LIA) maximum extent in the mid-18th century (Nesje et al., 2012).

3 Methods

3.1 Georadar

The ice patch was surveyed by a RAMAC georadar 23 September 2009 and 1 March 2012, using a high frequency antenna of 250 MHz. The dielectric constant of ice was set to be 3.2, giving a phase velocity of $168 \text{ m } \mu\text{s}^{-1}$. Georadar data and positioning data from the Global Navigation Satellite System (GNSS) were manually digitized to obtain a point dataset of ice thickness and bed topography. The point datasets were interpolated to get an ice thickness map and a digital terrain model (DTM) of the ice patch bed. Obvious artefacts caused by the interpolation technique were manually removed. A total of 40 independent control points gave an estimated standard deviation of 1.1 m, and a maximum error of 2.6 m. The control points were obtained by point measurements (GNSS) in the recently exposed area.

3.2 Laser scanning

The ice patch and surrounding terrain was scanned with an air-borne laser (Leica ALS70) on 17 September 2011. The company COWI AS, on assignment from Norwegian Water Resources and Energy Directorate, carried out the laser scanning and the processing of the data. The flight altitude was 10100-11800 feet (3078-3597 m a.s.l.). The area was scanned with 5 points m^2 . Quality controls and accuracy assessments revealed accuracy better than 0.1 m in surface elevation. Aerial photos were taken on the same day. These data were used to produce a high quality DTM and orthophotos of the ice patch surface and surrounding terrain. The DTM was resampled to a resolution of 1 m.

3.3 Mass balance and front measurements

Surface mass balance measurements of winter accumulation (snow depth at 20-60 sites and density at 1 site) and ablation (at 1-4 stakes) were made following standard methods for the melting seasons of 2010-2015 (Andreassen, 2011). Distance to the terminus was measured from two points outside the ice patch (Fig. 3a) in August or early September using a laser distance meter.

The extent of the Juvfonne ice patch was surveyed by foot with GNSS with a Topcon receiver mounted on a backpack and one reference receiver mounted in a fixed base point (Fig. 3a, Table 1). The GNSS data was processed with Topcon software TTOOLS version 8.

Surveys were done annually in August or September from 2010 to 2015, but the survey from 2012 was only done along the lower part due to snow conditions. Areal extent was also determined by digitising outlines from orthophotos from 2011 and from topographical maps from the Norwegian mapping authorities in 1981 and 2004. Furthermore, outlines from Landsat inventories from 1997 and 2003 were used (Andreassen et al., 2008; Winsvold et al., 2014). The accuracy of the differential GNSS are within 1m, the accuracy of the N50 within 5 m and the accuracy of the Landsat mapping within 30 m. The standard deviation in height of the GNSS measurements is on the range 10-20 cm giving ± 2 standard deviations of 0.6 m.

3.4 Meteorological measurements

Hourly meteorological data was obtained from the automatic weather station (AWS) at Juvvasshøe (1894 m a.s.l.). It is the highest official meteorological station in Norway, and is freely exposed and representative for this study, except for wind speed. The first station was set up in 1999 (Isaksen et al., 2003) and a new official weather station was established at the same site in June 2009. One additional station recording hourly snow depth was set up in autumn 2011 in front of Juvfonne (95 m from the eastern margin of the snowfield). Hourly data on snow depth is scarce in the high mountains in Scandinavia. Observed air temperature and wind speed on Juvvasshøe were compared against the 1971-2000 climatological normal based on interpolated air temperature data from seNorge (Engeset et al., 2004) and daily observations of wind speed from Fokstugu (973 m a.s.l.), 70 km NE of Juvvasshøe, which was the best nearby correlated meteorological station having long-time series.

A thermistor cable was installed in a 10 m deep borehole in 2009 to record ice temperatures. Temperatures were recorded every 3 hours until late September 2011 with an accuracy of 0.05

1 °C (1 standard deviation). The entire thermistor cable melted out in September 2014.
2 Additional thermistor measurements were made in the snow and ice at the onset of thaw in
3 spring 2010.

4 **3.5 Radiocarbon dating**

5 In May 2010, a 30 m long ice tunnel was excavated in the Juvfonne ice patch. During spring
6 2012, a new 70 m long tunnel was excavated into the central parts of the ice patch. The
7 tunnels were excavated with specially designed ice axes causing minimal disturbance to the
8 surrounding ice. The tunnels gave an excellent opportunity to verify the radar data and to
9 collect organic material and ice for radiocarbon dating. Dateable organic material is available,
10 but there are no continuous layers of organic material. Radiocarbons dating prior to 2012 are
11 published in (Nesje et al., 2012; Zapf et al., 2013; Ødegård et al., 2011). Conventional ^{14}C
12 ages were calibrated using OxCal v4.2.4 software (Bronk Ramsey and Lee, 2013) with the
13 IntCal13 calibration curve (Reimer et al., 2013).

14
15 The organic debris has been collected from the walls and below the floor of the ice tunnels (5
16 samples from the tunnel excavated in 2010 and 5 samples from the tunnel excavated in 2012 –
17 Table 2) and organic debris melting out at the front of which two datings are reported in this
18 paper. Nine additional datings were published by Nesje et al. (2012).

19 The recently developed method for radiocarbon dating of ice utilizes the organic carbon
20 fraction of carbonaceous aerosols scavenged from the atmosphere during snowfall and
21 embedded into the ice matrix (Jenk et al., 2009; Sigl et al., 2009; Uglietti et al., 2016). This
22 method was tested with 11 samples from Juvfonne in 2011 by comparing for the first time ^{14}C
23 ages determined from carbonaceous particles with ^{14}C ages conventionally obtained from
24 organic remains found in the ice (Zapf et al., 2013). The 2011 samples are JUV1 and JUV2
25 adjacent to the dated organic-rich layers in the 2010 tunnel and a surface sample JUV3 (Table
26 2). In summer 2015 five samples of clear ice were collected adjacent to the plant fragment
27 layer located just above the bed in the tunnel excavated in 2012 (JUV0, Table 2). All blocks
28 of ice ($\sim 20 \times 15 \times 10$ cm) were extracted with a pre-cleaned chainsaw and were subsequently
29 divided into smaller pieces. All ice blocks were transported frozen to Paul Scherrer Institute
30 (PSI, Switzerland), decontaminated in a cold room by removing the outer layer (0.3 mm) with

1 a pre cleaned stainless steel band saw and by rinsing the ice samples with ultra-pure water in a
2 class 100 clean room (Jenk et al., 2007).

3 Insoluble carbonaceous particles are filtered onto preheated quartz fibre filters (Pallflex
4 Tissuquartz, 2500QAO-UP) and combusted with a thermo-optical organic carbon/elemental
5 carbon (OC/EC) analyser (Model4L, Sunset Laboratory Inc., USA), using a well-established
6 protocol (Swiss_4S) for OC/EC separation (Zhang et al., 2012). Analyses of ^{14}C were
7 conducted using the 200 kV compact radiocarbon system 'MICADAS' at the University of
8 Bern (LARA laboratory), equipped with a gas ion source coupled to the Sunset instrument,
9 allowing measuring ^{14}C directly in CO_2 of 3-100 $\mu\text{g C}$ with an uncertainty level as low as 1%
10 (Ruff et al., 2010). Dates are given in calibrated ages BP (BP=1950 CE) including 1 sigma
11 errors (σ).

13 **4 Results**

14 **4.1 Ice thickness and ice layering**

15 The bed reflection was clearly seen in the radar plots (see example in Fig. 4). In addition the
16 ice layering was detected on most of the plots, probably due to density differences in the ice
17 layers (air bubbles) (Hamran et al., 2009) or organic layers. Georadar soundings from 2009
18 revealed a maximum ice thickness of 17-19 m (Ødegård et al., 2011). The near-surface
19 reflection horizons are nearly parallel to the present surface. At depth, curved reflection
20 horizons are observed. In the tunnels the curved layers can be directly observed forming a
21 distinct angular discontinuity with the surface-parallel ice layers (Fig. 5). The surface parallel
22 layers have melted away since 2009 in the central and southern parts of the ice patch (Fig 6).
23 The DTM obtained from laser scanning combined with the bottom topography from the
24 georadar gave a volume of 710,000 m^3 in late August 2011 (mean thickness 5.6 m). The
25 surface of Juvfonne in September 2011 was the reference surface for the depth map (Fig. 3b).
26 The maximum depth was 16 m close to the inner part of ice tunnel excavated in 2012. In this
27 area the surface slope is about 18 degrees.

4.2 Mass balance, front changes and areal extent

Only one of the mass balance stakes (J2) existed continuously from spring 2010 to spring 2015 (Figs. 7 and 8). Stake J2 is in the central part of the ice patch (Fig. 3a).

Snow sounding measurements (N=232) range from 0.6-4.8 m over the period 2010-2015. Mean snow depth is 2.6 m (1.2 m w.e.). Some years show a pattern where most snow accumulates on the leeward side of the prevailing wind the previous winter, but this is not consistent. Inter annual variation accounts for 66%. The accumulation was further investigated by analysing the deviation from mean each year. This dataset contains a significant trend with increased accumulation towards the front (Fig. 3c). The difference between the upper central area and the front is 0.2 m w.e (Fig. 3c), which corresponds to approx. 20% increase in accumulation.

The total mass loss is measured to 10 m of ice at the site of the thermistor measurements (Fig. 3a). The 10-metre thermistor cable installed on the 29 October 2009 melted out in mid-September 2014. The total mass loss at stake J2 was 10.5 m w.e. during the same period. Elevation changes from September 2011 to September 2014 are shown in Fig. 3d. These results are based on the laser scanning in 2011 and differential GNSS-tracking in 2014. The measurements show a highly significant asymmetric pattern with close to zero surface elevation changes in the western part and surface lowering of 3-5 m in the eastern and central part of the ice patch. This strong gradient is measured over a distance of just 200 m at approximately the same altitude. The part with most negative change has more than average accumulation.

Front change measurements started in 2009 at JF1 and in 2010 at JF2 (Fig. 9). The measurements revealed that Juvfonne retreated in all years except in 2012 and 2015 where the ice patch increased its size due to excessive snow that formed a thin ice and snow layer around the margin. The total retreat 2009-2014 is -52 m measured from JF1 and over 2010-2014 the mean change is 44 m (-51m from JF1 and -38 m from JF2).

The annual extent measurements (2010-2015) show area fluctuations of the margin, varying from 0.101 km² (9 September 2014) to a maximum of 0.186 km² on 11 September 2015 (Table 1). The extent measurements show that the ice patch shrinks and grows along the whole margin. Furthermore, observations in field show that the ice is very thin along the margins. In 2015, seasonal snow covered the entire margin, and the measured area of 0.186 km² is thus only to be considered a maximum extent, not the actual ice patch area.

4.3 Climate parameters

Air temperature and wind speed at Juvvasshøe for the period 2000-2015 are outlined in Fig. 10 a-b over the ablation season (June-September). The mean June-September air temperature in this period is 3.2 °C (1.0 °C above the 1971-2000 mean). Air temperatures, near-ground surface temperatures and frequency of days with daily mean air temperature above 0 °C (the two latter are not shown in Fig. 10) are high in summers 2002, 2003, 2006, 2011 and 2014, and especially 2006. Observations from nearby weather stations with long climate series reported record-breaking temperatures in late summer and autumn 2006. In the investigation period 2009-2015 the coldest summer was 2012, which was the only summer below the 1971-2000 mean (Fig. 10).

Due to the sheltered setting of Juvfonne compared to the meteorological stations, strong breeze (wind speed above 10.8 ms⁻¹) was used as a lower limit to get sufficient high wind speeds for effective and enhanced turbulent fluxes at Juvfonne. In general there is a high frequency (35-58 days per season) of strong breeze during the period 2009-2015 (Fig. 10b). Comparing wind data from the AWS at Fokstugu indicates two to three times more frequent strong wind than 1971-2000 mean during the investigation period. Observed incoming short- and longwave radiation from Juvvasshøe (not shown) show no clear patterns related to single summers, but 2011 stands out as the summer with greatest incoming long wave radiation.

For snow accumulation or abrasion on ice patches wind speed and wind direction is crucial (Dadic et al., 2010; Lehning et al., 2008). There are great variations from year to year in respect to frequency of strong gale and wind direction. During the two stormiest winters 2011-12 and 2013-14, the frequency of strong gale was 15.7 % and 17.3 %, respectively (Fig. 11).

4.4 Snow measurements and modelling

The automatic snow depth observations in front of Juvfonne show great hourly to daily variability and there is distinct different pattern of snow accumulation between the four winter seasons (Fig. 12). The greatest increase in snow depth during early and mid-winter in all years is related to storm events. This is also the case for strong snow depth decrease events (mainly due to wind scouring). Comparing the observed and estimated snow depths (which don't take into account redistribution of snow by wind), it is clear that much of the accumulation is not correlated with precipitation (Fig. 12). The snow depth for Juvfonne was obtained from a

precipitation/degree-day model operating on 1×1 km² developed for a web-based system (<http://senorge.no/>) for producing daily snow maps for Norway (Engeset et al., 2004; Saloranto, 2012). A similar poor correlation ($r^2=0.24$) is also found for very small glaciers in the Alps (Huss and Fischer, 2016)

The observed melt in central parts (J2) was compared with a degree-day model using typical values calculated from nearby glaciers (Fig. 7a) (Laumann and Reeh, 1993). This modelling shows a quite good fit except the 2010 season. In this season, the summer balance was about twice the outcome of the degree-day model.

4.5 Temperature of ice and permafrost

Temperature measurements in Juvfonne reveal 10-m depth ice temperature in the range of -2 to -4 °C (Fig. 13). The ice and snow temperature results show that the Juvfonne ice patch is cold-based and underlain by permafrost. The measurements at 5-10 m depth in the ice are similar to the measurements in the nearby permafrost borehole at Juvvasshøe (Fig. 13). In spring, the melt water percolates and refreezes in the snowpack until the snow is isothermal at a temperature close to 0°C (Fig. 14). There is cold ice below the level of meltwater percolation, which means that there is a heat flow into the ice gradually decreasing during the melt season. Because of this heat flow superimposed ice forms at the level of impermeable ice, generally less than 0.1 m/year.

4.6 Radiocarbon dating

The AMS radiocarbon dating obtained from organic-rich layers and from carbonaceous aerosols embedded in clear ice in the Juvfonne ice patch shows ages spanning from modern at the surface to ca. 7600 cal. years BP at the bottom (clear ice below the basal organic-rich layer), thus showing that Juvfonne has existed continuously during the last ~7500 years. So far, the basal ice in Juvfonne is the oldest dated ice in mainland Norway (Table 2).

In the tunnel opened in 2010 the AMS radiocarbon dating of organic matter embedded in the ice shows modern age in the top layer at the entrance, and ages ranging from 3075-3168 cal.

1 years BP to 963-1005 cal. years BP inside the tunnel. These results were previously published
2 in Nesje et al. (2012) and recalibrated for this study (Table 2 and Fig. 15).

3 In the tunnel opened in 2012 the AMS radiocarbon dating of five organic layers embedded in
4 the ice about 70 m from the margin of the ice patch, yielded dates in chronological order from
5 the base upwards, ranging from 6555-6660 cal. years BP at the base to 1929-2002 cal. years
6 BP in the ceiling of the ice tunnel, approximately 2.8 m above the tunnel floor. The organic
7 debris that yielded the oldest age was collected from the innermost part of the ice tunnel,
8 about 0.4 m above the bed. The layer where the sample was retrieved could be followed close
9 to the bed in the inner parts of the tunnel. The carbon dates on carbonaceous aerosols were
10 sampled at the same location to the side and below the plant fragment layer. The oldest dating
11 is 7476-7785 cal. years BP. The position of the sample site in the 2012 tunnel is marked on
12 Fig. 3a.

13 In the autumn 2014, two *in-situ Polytrichum* moss mats melted out along the margin of
14 Juvfonne south of the ice tunnel excavated in 2010. AMS radiocarbon dates of the two moss
15 mats indicate that the moss was killed by the expanding margin of the ice patch about 2000
16 years ago (1951-1896 cal. years BP - Poz-66166 and 1945-1882 cal. years BP - Poz-66167).
17 Thus, the minimum extent of the southeastern part of the ice patch observed in September
18 2014 is most likely the smallest in 2000 years.

19 With the exception of one identified outlier, the results obtained from dating of carbonaceous
20 aerosol particles in the ice could reproduce the expected ages very well (Zapf et al., 2013).
21 This gives confidence that the age of organic debris in the ice is similar to the surrounding ice.
22 In fig. 16 radiocarbon datings from both ice tunnels are plotted according to vertical distance
23 from bed.

24 25 **5 Discussion**

26 The discussion focuses on the value of this research in the context of the long-term objective
27 to develop models of mass balance and thermal regime on Holocene time scale at ice patches
28 and surrounding terrain.

29 The discussion is organised in four sections: (1) the mass balance, (2) thermal regime, (3) ice
30 layering and deformation on Holocene time scale and (4) the environmental processes
31 relevant to artefact displacement and preservation.

5.1 The mass balance

Perennial ice patches are, due to their existence, located at sites with close to long-term zero mass balance. The inter-annual variability in summer and winter balance could be considerable, but the long-term changes in mass must be close to zero as long as they do not disappear or develop into a glacier. The 6-year record of mass balance gives some insight into the spatial and temporal variability of the mass balance.

The snow accumulation during the 6-year period (2010-2015) shows increased accumulation towards the front of the ice patch. This is probably a response to increased melt, which will increase the snow accumulation at the leeward side of prevailing westerly winds.

Along the outer rim of Juvfonne, the surface altitude changes (negative mass balance) vary between less than 1m to nearly 5m within a 200 m distance at same altitude over a period of 3 years (Fig. 3d). Field data is consistent with the interpretation of increased melting due to sensible and latent heat fluxes. Micro-meteorological investigations by Mott et al. (2011) of processes driving snow ablation in an alpine catchment show that advection of sensible heat cause locally increased ablation rates at the upwind edges of snow patches.

The 2010 anomaly in the summer balance (Fig. 7a) is most likely related to increased melt during periods with strong south and southeasterly winds (unsheltered direction for Juvfonne) combined with relatively high air temperatures and high relative humidity causing enhanced turbulent fluxes. Extreme melt was observed in early-mid August. The warmest 10-day period in 2010 was 8-18 August. Median wind speed was 3.4 m/s from SE and humidity 79.5% at the meteorological station 750 m from the ice patch. This 2010 anomaly is probably the reason for the asymmetric net balance of Juvfonne (Fig. 6). Exceptionally large melt episodes have been reported from the Central Cascade Mountains of Oregon where snow melt were enhanced by strong wind, high air temperature and high humidity (Marks et al., 1998). At higher unsheltered sites 60-90% of the energy for snowmelt came from sensible and latent heat exchanges, while it was only about 35% at more sheltered sites. Recently similar extreme melt events have been reported from the southern and western part of Greenland ice sheet in July 2012, where nonradiative energy fluxes (sensible, latent, rain, and subsurface collectively) dominated the ablation area surface energy budget during multiday episodes (Fausto et al., 2016).

The snow recording from the station in front of Juvfonne (95 m from the front) clearly illustrates the complexity of snow accumulation in this environment. In front of Juvfonne,

1 abrupt changes in snow depth within hours dominate the series, causing great day-to-day
2 variability. These changes seem to be mainly driven by the rate of wind speed and wind
3 direction. Single storm events with westerly winds could account for almost 50% of the
4 winter accumulation in less than 24 hours, like the storm February 7-8 in 2015 (Fig. 12, 2014-
5 15). Spring snow accumulation with insignificant wind drift could also influence mass
6 balance, like the period from early April to mid May 2012 where more than 40 cm of snow
7 accumulated (Fig. 12, 2011-2012).

8 **5.2 Ground and ice thermal regime**

9 The temperature measurements at Juvfonne show that there is sufficient melt water to bring
10 the permeable snowpack to an isothermal condition within a few weeks in early summer (Fig.
11 13). Below the seasonal snowpack, the ice remains cold during the summer with temperatures
12 on the range -2 - -4°C at 5-10 m depth (Fig. 13). In Norway most glaciers are considered to be
13 temperate, although measurements are available for only a few glaciers (Andreassen and
14 Winsvold, 2012). Recent observations from nearby glaciers in Jotunheimen, reveal that at the
15 lower parts of Storbreen the winter cold wave is removed during summer, but remained at
16 Hellstugubreen and Gråsubreen (Sørdal, 2013; Tachon, 2015). The temperature measured
17 close to the equilibrium line at Hellstugubreen (-1°C) and Gråsubreen (-2°C) were warmer
18 than the temperature measured at similar depths at Juvfonne (-3°C).

19 Juvfonne consists of cold ice surrounded by permafrost terrain (Fig. 13). Perennial ice patches
20 can be used as indicators of local (mountain) permafrost conditions (Imhof, 1996; Kneisel,
21 1998). The physical background is that their ice cannot warm above 0°C in summer, but cool
22 down far below 0°C during the cold season. Based on this argument there is good reason to
23 suggest that long-term perennial ice patches like Juvfonne indicate permafrost directly
24 beneath them. Holocene permafrost modelling (Lilleøren et al., 2012) suggest that permafrost
25 survived the highest areas of the Scandinavian mountains during the Holocene thermal
26 maximum (HTM), and thus permafrost ice could be of Pleistocene age. Radiocarbon dates
27 from Juvfonne show that the deepest central part of the ice patch contains carbonaceous
28 particles embedded in the ice 7476-7785 cal. years BP (JUV0_B - Table 2). This is a strong
29 indication that Juvfonne has existed continuously since mid-Holocene, and the dating of the
30 ice could offer strongly needed validation of Holocene permafrost models. Juvfonne could
31 contain older ice, and it is most likely that ice patches at higher altitude contains older ice.

5.3 Ice layering and deformation on Holocene time scale

The observed ice layers almost certainly represent surface of isochronic deposition. Within both ice tunnels in Juvfonne there are several organic/debris layers of uncertain origin. From the appearance of these layers, it is probably wind or water transported material or reindeer droppings. The organic layers are horizontally continuous over a few meters. There is reasonable correlation between the age of the clear ice and the age of the organic layers (Zapf et al., 2013). Contamination is not likely in the clear ice samples, which gives confidence in the dating of the ice stratigraphy. This is necessarily not the case at other ice patches, where surface processes or microbial activity may contaminate organic material exposed at the surface.

The ice deformation on Holocene time scale is difficult to calculate based on the available data. In the central parts of the ice patch, an estimate of maximum basal shear stress is on the range of 30-40 kPa (surface slope 17°, depth 12-16 m, laminar flow). Adding 5 m to the depth will increase the basal shear stress to 45-55 kPa for the central part. The latter is probably close to the range for the last decades. Calculation of deformation based on a Glen type flow law will be highly sensitive to the chosen stress exponent (Glen, 1955). Using a softness parameter $A=2.4 \cdot 10^{-15} \text{ s}^{-1} \text{ kPa}^{-3}$ based on an ice temperature of -2 °C from Table 5.2 in Paterson (1994) and a stress exponent of $n=2$ (Duval et al., 2000) gives a surface velocity of 2.3 m/1000*years (surface slope 17°, depth 19 m, laminar flow). A likely situation for the LIA (surface slope 15°, depth 45-60 m) gives an estimate of 25-60 m/1000*years assuming a cold based glacier (Fig. 17). These calculations are uncertain, but suggest that a cumulative deformation of ice over millennia could explain the observed curved layering in the basal layer of the ice patch (Fig. 4). The possibility of cumulative ice deformation on a time scale of several millennia makes it difficult to relate the present thickness and slope of these layers to previous thickness of the ice patch.

5.4 Artefact displacement and preservation

From a cultural management perspective, there is particular interest in developing methods to identify sites of interest (Rogers et al., 2014) and a better understanding of the environmental threats (Callanan, 2015). The environmental threats are mainly related to sub-aerial exposure

1 of artefacts. Especially leather artefacts, textiles and steering feathers of arrows are exposed to
2 movement and decomposition short time after melt out. Wooden objects are more resistant.

3 The artefacts found at Juvfonne are in permafrost terrain surrounding the ice patch, most of
4 them are found in the front of the ice patch within a few tens of meters. The wooden artefacts
5 range from 250-900 CE. Even during the extreme minimum in September 2014 (Fig. 6) there
6 are no observations of artefacts melting out within the ice.

7 The exposure time to physical processes and microbial activity is critical to artefact
8 decomposition. At Juvfonne, there is a gradual increase in the ground exposure time
9 depending on snow accumulation and melt over millennia. The oldest ice found so far is
10 7476-7785 cal. years BP (JUV0_B - Table 2). At the eastern edge AMS radiocarbon dates
11 show that the moss mats were covered (killed) by the expanding snowfield about 2000 years
12 ago (Table 2, Poz-56952). Lichenometry indicates that the front of Juvfonne extended ~250 m
13 from its present position during the LIA maximum in the mid-18th century (Nesje et al.,
14 2012). A photo of Juvfonne from around 1900 shows the front close to the expected LIA
15 extent (Fig. 17). These results constrain the extent of the ice patch since the mid-Holocene,
16 but temporal and spatial variability need to be considered to assess the actual exposure time of
17 artefacts.

18 Several radiocarbon dates of the top layer in 2010 (Fig. 4) show modern age. This means that
19 artefacts found at Juvfonne have been sub-aerially exposed after the LIA but prior to 2009.
20 Thus, the dating and position of artefacts cannot be used directly to reconstruct previous ice
21 patch extent.

22 Juvfonne and surrounding terrain is an active environment in terms of geomorphological
23 processes. In particular, during the extreme melting in autumn 2014 several small
24 accumulations of organic material/debris occurred at the upper margin of the ice patch.
25 Within a few days, melt water moved this material to the front of the ice patch. Downslope
26 movement of artefacts by melt water is certainly possible at Juvfonne. Finds at other ice
27 patches in Jotunheimen supports this interpretation, where different pieces of the same
28 artefact were found along the direction of steepest slope. Textiles and leather objects are more
29 likely transported by wind, and preservation at its original position is less likely. There are no
30 finds of textiles or leather objects at Juvfonne.

31

6 Conclusions and future perspectives

The exploratory analyses of field data from Juvfonne show for the first time the geoscience research potential of ice patches in Scandinavia. The results give new insights into their age, internal structure, mass balance and climate sensitivity, and have taken the state of knowledge to level where models can be designed.

These are the main conclusions from the analysis of field data:

- Ice stratigraphic characteristics and radiocarbon dating strongly suggest that the Juvfonne ice patch was small or absent during Holocene thermal maximum, but existed continuously since ca. 7600 cal. years BP (the late Mesolithic period) without disappearing. This is the oldest dating of ice in mainland Norway.
- A 6-year record of mass balance measurements shows a strong negative balance. The total mass loss at one site was 10.5 m w.e. Elevation changes are highly asymmetric over short distances, from close to zero to surface lowering of several meters. There is a significant increase in snow accumulation towards the front of approx. 20% compared to the upper central area. The winter balance is poorly correlated with winter precipitation. One single storm event may contribute significantly to the winter balance.
- Temperature measurements of the ice in Juvfonne reveal colder ice than what is found at similar depths close to the equilibrium line of nearby polythermal glaciers. There is sufficient melt water to bring the permeable snowpack to an isothermal state within a few weeks in early summer. Below the seasonal snowpack, at 5-10 m depth, the ice remains cold with temperatures between -2 and -4°C. The cold ice is surrounded by permafrost terrain having similar ground temperatures.
- Geophysical investigations show a clear stratification. The observed ice layers almost certainly represent surface of isochronic deposition. At depth, curved reflection horizons are observed consistent with cumulative ice deformation over millennia.
- Ice deformation and surface processes (i.e. wind and melt water) may have caused significant displacement of artefacts from their original position.
- Since the surface ice shows modern age artefacts melted out in front of Juvfonne since 2009 have been sub-aerially exposed after the LIA but prior to 2009. Thus, the dating

1 and position of artefacts cannot be used directly to reconstruct previous ice patch
2 extent.

3

4 The radiocarbon datings show that Juvfonne is robust to climate change, even on a Holocene
5 timescale. The datings indicate a slow build-up over a period of 8000 years. The survival of
6 relatively thin ice over a long period is a good documentation of the well-known mass balance
7 feedback mechanisms of ice patches. The datings of mass mats appearing at the southeastern
8 edge of Juvfonne in September 2014 suggest the smallest ice patch in ~2000 years. These
9 field data constrain the Holocene development of Juvfonne, but care should be taken in the
10 interpretation. Radiocarbon datings of the ice layers only show the timing of minima in
11 volume.

12 Perennial ice patches are, due to their existence, areas with close to long-term zero mass
13 balance similar to the zone close to the ELA of glaciers. However, there are obvious
14 differences between ice patches and glaciers. The accumulation processes are to a variable
15 degree dependent on surrounding topography and the topography of the ice patch itself. One
16 possible future approach is field observations in combination with simulations of the wind
17 field to obtain the necessary spatial and temporal resolution to model the snow accumulation
18 during storm events. The wind field with high spatial and temporal resolution is also needed
19 to calculate the turbulent fluxes.

20 Ice patches are in the transition zone between seasonal snow cover and perennial snow/ice.
21 This interaction needs to be addressed since ice patches could be influenced by advective heat
22 transfer in summer. The melt anomaly in 2010 is probably related to periods of strong
23 southeasterly winds, high air temperatures and high relative moisture boosting the turbulent
24 fluxes at the upwind edge. The time series of mass balance at Juvfonne is too short to study
25 the long-term effect of melt anomalies.

26 The possibility of cumulative deformation of ice on a Holocene time scale makes it difficult
27 to relate the present thickness and slope of theses layer to previous thickness of the ice patch.
28 Maximum ice volume was reached during LIA, when Juvfonne probably developed into a
29 cold based glacier with significant internal deformation.

30

7 Data availability

The ice thickness and point mass balance data of Juvfonne are submitted to the World Glacier Monitoring Service (WGMS) to their Glacier Thickness Database (GlaThiDa) and Fluctuations of Glaciers Database (FoG). The snow accumulation data are included in the supplement. Meteorological data for stations Juvvasshøe (15270) and Fokstugu (16610) are available for free download from the climate database of the Norwegian Meteorological Institute, eKlima (<http://eklima.met.no/>).

Acknowledgements. We thank the archaeologists Lars Pilø and Espen Finstad for valuable comments and discussions related to artefact displacements and Dag Inge Bakke at Mimisbrunnr Klimapark 2469 for support in the field. Professor Emeritus Wilfried Haeberli and Professor Bernd Etzelmüller gave useful comments to an earlier version of the manuscript and are gratefully acknowledged. We thank two anonymous reviewers for precise feedback, which greatly improved the manuscript.

References

- Andreassen, L. M.: Glaciological investigations in Norway in 2010 - Juvfonne, NVE report 3, B. Kjølmoen (ed), 54-57 pp., 2011.
- Andreassen, L. M., Elvehøy, H., Kjølmoen, B., Engeset, R. V., and Haakensen, N.: Glacier mass-balance and length variations in Norway, *Ann Glaciol*, 42, 317-325, 2005.
- Andreassen, L. M., Paul, F., Kääb, A., and Hausberg, J. E.: Landsat-derived glacier inventory for Jotunheimen, Norway, and deduced glacier changes since the 1930s, *The Cryosphere*, 2, 131-145, 2008.
- Andreassen, L. M. and Winsvold, S. H.: Inventory of Norwegian Glaciers, 236 pp. pp., 2012.
- Andrews, T. D. and Mackay, G.: The Archaeology and Paleocology of Alpine Ice Patches: A Global Perspective, *ARCTIC*, 65, 4 pp., 2012.
- Bakke, J., Dahl, S. O., Paasche, Ø., Riis Simonsen, J., Kvisvik, B., Bakke, K., and Nesje, A.: A complete record of Holocene glacier variability at Austre Okstindbreen, northern Norway: an integratd approach, *Quaternary Science Reviews*, 29, 1246-1262, 2010.
- Bronk Ramsey, C. and Lee, S.: Recent and Planned Developments of the Program OxCal, *Radiocarbon*, 55, 2013.
- Brunswig, R. H.: Risks and Benefits of Global Warming and the Loss of Mountain Glaciers and Ice Patches to Archeological, Paleoclimate, and Paleoecology Resources, *Ecological Questions*, 20, 99-108, 2014.
- Callanan, M.: Managing the frozen heritage: Some challenges and responses, *Quaternary International*, in press, 8 pp., 2015.
- Callanan, M.: Northern Snow Patch Archaeology, Oxford2010.
- Ceruti, C.: Human bodies as objects of dedication at Inca mountain shrines, north-western Argentina, *World Archaeology*, 36, 103-122, 2004.
- Curry, A.: Racing the thaw, *Science*, 346, 157-159, 2014.
- Dadic, R., Mott, R., Lehning, M., and Burlando, P.: Wind influence on snow depth distribution and accumulation over glaciers, *J Geophys Res*, 115, 8 pp., 2010.
- Dixon, E. J., Callanan, M., Hafner, A., and Hare, G. P.: The Emergence of Glacial Archaeology, *Journal of Glacial Archaeology*, 1, 1-9, 2014.
- Dixon, J., Manley, W. E., and Lee, C. M.: The emerging archaeology of glaciers and ice patches, *American Antiquity*, 70, 129-143, 2005.
- Duval, P., Arnaud, L., Brissaud, M., Montagnat, M., and de la Chapelle, S.: Deformation and recrystallization processes of ice from polar ice sheets, *Annals of Glaciology*, 30, 83-87, 2000.
- Engeset, R. V., Tveito, O. E., Alfnes, E., Mengistu, Z., Udnæs, H.-C., Isaksen, K., and Førland, E. J.: Snow Map System for Norway, Tallinn, Estonia2004.
- Essery, E., Ganger, R., and Pomeroy, J.: Boundary-layer growth and advection of heat over snow and soil patches: modelling and parameterization, *Hydrol. Processes*, 20, 953-967, 2006.

- 1 Eveland, J. W., Gooseff, M. N., Lampkin, D. J., Barrett, J. E., and D., T.-V. C.: Seasonal
2 controls on snow distribution and aerial ablation at the snow patch and landscape scales
3 McMurdo Dry Valleys, Antarctica, *The Cryosphere*, 7, 917–913, 2013.
- 4 Farbrot, H., Hipp, T., Etzelmuller, B., Isaken, K., Ødegård, R. S., Schuler, T. V., and
5 Humlum, O.: Air and Ground Temperatures Variations Observed along Elevation and
6 Continentality Gradients in Southern Norway, *Permafrost Periglacial Processes*, doi:
7 10.1002/ppp.733, 2011. 2011.
- 8 Farnell, R., Hare, G. P., Blake, E., Bowyer, V., Schweger, C., Greer, S., and Gotthardt, R.,
9 2004. . *Arctic* 57(3), 247–259.: Multidisciplinary investigations of alpine ice patches in
10 Southwest Yukon, Canada: paleo-environmental and paleobiological investigations, *ARCTIC*,
11 57, 247-259, 2004.
- 12 Fausto, R. S., van As, D., Box, J. E., Colgan, W., Langen, P. L., and Mottram, R. H.: The
13 implication of nonradiative energy fluxes dominating Greenland ice sheet exceptional
14 ablation area surface melt in 2012, *Geophys. Res. Lett.*, 43, 10 pp., 2016.
- 15 Finstad, E. and Vedeler, M.: En bronsealdersko fra Jotunheimen, *Viking*, 71, 61-70, 2008.
- 16 Fujita, K., Hiyama, K., Iida, H., and Ageta, Y.: Self-regulated fluctuations in the ablation of a
17 snow patch over four decades, *Water Resour. Res.*, 46, 9, 2010.
- 18 Fukui, K.: Permafrost and surface movement of an active protalus rampart in the Kuranosuke
19 Cirque, the Northern Japanese Alps, *Permafrost Conference*, Zurich, 2003.
- 20 Fukui, K. and Iida, H.: Flow of the ice body in the Gozenzawa perennial snow patch, the
21 Tateyama Mountains, central Japan, 2011.
- 22 Gislås, K., Etzelmuller, B., Farbrot, H., Schuler, T. V., and Westermann, S.: CryoGRID 1.0:
23 Permafrost Distribution in Norway estimated by a Spatial Numerical Model, *Permafrost*
24 *Periglacial Processes*, 24, 2-19, 2013.
- 25 Gislås, K., Westermann, S., Schuler, T. V., Melvold, K., and Etzelmuller, B.: Small-scale
26 variation of snow in a regional permafrost model, *The Cryosphere Discuss.*, 9, 6661-6696,
27 2015.
- 28 Glazirin, G. E., Kodama, Y., and Ohata, T.: Stability of drifting snow-type perennial snow
29 patches, *Bull. Glaciol. Res.*, 21, 1-8, 2004.
- 30 Glen, J. W.: The creep of polycrystalline ice, *Proc. R. Soc. Ser. A*, 228, 519-538, 1955.
- 31 Grosjean, M., Suter, P. J., Trachsel, M., and Wanner, H.: Ice-borne prehistoric finds in the
32 Swiss Alps reflect Holocene glacier fluctuations, *J. Quat. Sci.*, 22, 203-207, 2007.
- 33 Haeberli, W., Frauenfelder, R., Kääb, A., and Wagner, S.: Characteristics and potential
34 climatic significance of “miniature ice caps” (crest- and cornice-type low-altitude ice
35 archives), *J GLACIOL*, 50, 129-136, 2004.
- 36 Hamran, S.-E., Øyan, M. J., and Kohler, J.: UWB radar profiling reveals glacier facies,
37 Granada, Spain2009.
- 38 Hansen, J. P. H., Meldgaard, J., and Nordquist, J.: Qilakitsoq. De Grønlandske mumier fra
39 1400-tallet, Nuuk and Copenhagen: Grønlands Landsmuseum/Christian Ejlers' forlag, 1985.
- 40 Hare, G. P., Thomas, C. D., Topper, T. N., and Gotthardt, R. M.: The archaeology of Yukon
41 ice patches: New artifacts, observations, and insights, *ARCTIC*, 65, SUPPL. 1, 118-135,
42 2012.

1 Harris, C., Arenson, L. U., Christiansen, H. H., Etzelmuller, B., Frauenfelder, R., Gruber, S.,
2 Haeberli, W., Hauck, C., Holzle, M., Humlum, O., Isaksen, K., Kaab, A., Kern-Lutschg, M.
3 A., Lehning, M., Matsuoka, N., Murton, J. B., Nozli, J., Phillips, M., Ross, N., Seppala, M.,
4 Springman, S. M., and Muhll, D. V.: Permafrost and climate in Europe: Monitoring and
5 modelling thermal, geomorphological and geotechnical responses, *Earth Sci. Rev.*, 92, 117-
6 171, 2009.

7 Hauck, C., Isaksen, K., Vonder Mühll, D., and Sollid, J. L.: Geophysical surveys designed to
8 delineate the altitudinal limit of mountain permafrost: an example from Jotunheimen,
9 Norway, *Permafrost Periglac.*, 15, 191-205, 2004.

10 Hipp, T., Etzelmuller, B., Farbrot, H., Schuler, D. V., and Westermann, S.: Modelling
11 borehole temperatures in Southern Norway – insights into permafrost dynamics during the
12 20th and 21st century, *Cryosphere*, 6, 553-571, 2012.

13 Huss, M. and Fischer, M.: Sensitivity of Very Small Glaciers in the Swiss Alps to Future
14 Climate Change, *Front. Earth Sci.*, 4, 17 pp., 2016.

15 Imhof, M.: Modelling and Verification of the Permafrost Distribution in the Bernese Alps
16 (Western Switzerland) *Permafrost Periglac.*, 7, 267-280, 1996.

17 Isaksen, K., Hauck, C., Gudevang, E., Ødegård, R. S., and Sollid, J. L.: Mountain permafrost
18 distribution on Dovrefjell and Jotunheimen, southern Norway, based on BTS and DC
19 resistivity tomography data, *Norsk Geografisk Tidsskrift*, 56, 122-136, 2002.

20 Isaksen, K., Heggem, E. S. F., Bakkehøi, S., Ødegård, R. S., Eiken, T., Etzelmüller, B., and
21 Sollid, J. L.: Mountain permafrost and energy balance on Juvvasshøe, southern Norway, In
22 *Proceedings Volume 1, Eight International Conference on Permafrost*, Zurich, Switzerland,
23 21–25 July, 2003. 467-472, 2003.

24 Isaksen, K., Ødegård, R. S., Etzelmuller, B., Hilbich, C., Hauck, C., Farbrot, H., Eiken, T.,
25 Hygen, H. O., and Hipp, T.: Degrading mountain permafrost in southern Norway - spatial and
26 temporal variability of mean ground temperatures 1999-2009, *Permafrost Periglacial*
27 *Processes*, 22, 361-377, 2011.

28 Jenk, T. M., Szidat, S., Bolius, D., Sigl, M., Gäggeler, H. W., Wacker, L., Ruff, M., Barbante,
29 C., Boutron, C. F., and Schwikowski, M.: A novel radiocarbon dating technique applied to an
30 ice core from the Alps indicating late Pleistocene ages, *J. Geophys. Res.*, 114, 2009.

31 Jenk, T. M., Szidat, S., Schwikowski, M., Gaggeler, H. W., Wachter, L., Synal, H.-A., and
32 Sauer, M.: Microgram level radiocarbon (14C) determination on carbonaceous particles in
33 ice, *Nuclear Instruments and Methods in Physics Research B* 259, 518-525, 2007.

34 Kawasaki, K., Yamada, T., and Wakahama, G.: Investigation of internal structure and
35 transformational processes from firn and ice in a perennial snow patch, *Ann Glaciol.*, 18, 117-
36 122, 1993.

37 Kjølmoen, B., Andreasse, L. M., Elvehøy, H., Jackson, M., and Giesen, R. H.: Glaciological
38 investigations in Norway 2010, 106 pp. pp., 2011.

39 Kneisel, C.: Occurrence of surface ice and ground ice/permafrost in recently deglaciated
40 glacier forefields, St. Moritz area, Eastern Swiss Alps, Yellowknife, Canada 1998, 575-581.

41 Laumann, T. and Reeh, N.: Sensitivity to climate change of the mass balance of glaciers in
42 southern Norway, *J GLACIOL.*, 39, 656-665, 1993.

1 Lee, C. M.: Withering snow and ice in the mid-latitudes: A new archaeological and
2 paleobiological record for the Rocky Mountain region, ARCTIC, 2012. 165-177, 2012.

3 Lehning, M., Löwe, H., Ryser, M., and Raderschall, N.: Inhomogeneous precipitation
4 distribution and snow transport in steep terrain, Water Resour. Res., 44, 19 pp., 2008.

5 Lilleøren, K., Etzelmüller, B., Schuler, D. V., Gissnås, K., and Humlum, O.: The relative age
6 of mountain permafrost - estimation of Holocene permafrost limits in Norway Global Planet.
7 Change, 92-93, 209-223, 2012.

8 Marks, D., Kimball, J., Tingey, D., and Link, T.: The sensitivity of snowmelt processes to
9 climate conditions and forest cover during rain-on-snow: a case study of the 1996 Pacific
10 Northwest flood, Hydrol. Processes, 12, 1569-1587, 1998.

11 Matthews, J. A. and Dresser, P. Q.: Holocene glacier variation chronology of the
12 Smørstabbtinden massif, Jotunheimen, southern Norway, and the recognition of century- to
13 millennial-scale European Neoglacial events, The Holocene, 18, 181-201, 2008.

14 Meulendyk, T., Moorman, B. J., Andrews, T. A., and Mackay, G.: Morphology and
15 Development of Ice Patches in Northwest Territories, Canada, ARCTIC, 65, SUPPL. 1, 43-
16 58, 2012.

17 Morris, E. M.: Turbulent Transfer over Snow and Ice, Journal of Hydrology, 105, 205-223,
18 1989.

19 Mott, R., Daniels, M., and Lehning, M.: Atmospheric Flow Development and Associated
20 Changes in Turbulent Sensible Heat Flux over Patchy Mountain Snow Cover, J
21 Hydrometeorol, 16, 1315-1340, 2015.

22 Mott, R., Egli, L., Grunewald, T., Dawes, N., Manes, C., Bavay, M., and Lehning, M.:
23 Micrometeorological processes driving snow ablation in an Alpine catchment, The
24 Cryosphere, 5, 1083-1098, 2011.

25 Nesje, A.: Latest Pleistocene and Holocene alpine glacier fluctuations in Scandinavia. ,
26 Quaternary Science Reviews, 28, 2119-2136, 2009.

27 Nesje, A., Pilø, L. H., Finstand, E., Solli, B., Wangen, V., Ødegård, R. S., Isaken, K., Støren,
28 E., Bakke, D. I., and Andreassen, L. M.: The climatic significance of artefacts related to
29 prehistoric reindeer hunting exposed at melting ice patches in southern Norway, The
30 Holocene, 22, 485-496, 2012.

31 Paterson, W. S. B.: The Physics of Glaciers, Pergamon, 1994.

32 Pohl, S., Marsh, P., and Liston, G. E.: Spatial-Temporal Variability in Turbulent Fluxes
33 during Spring Snowmelt, ARCT ANTARCT ALP RES, 38, 136-146, 2006.

34 Reckin, R.: Ice Patch Archaeology in Global Perspective: Archaeological Discoveries from
35 Alpine Ice Patches Worldwide and Their Relationship with Paleoclimates, Journal of World
36 Prehistory, 26, 63 pp., 2013.

37 Reimer, P. J., Barad, E., Baykuss, A., Beck, J. W., Blackwell, P. G., Bronk Ramsey, C., Buck,
38 C. E., Cheng, H., Edwards, R. L., Friedrich, M., Grootes, P. M., Guilderson, T. P.,
39 Haflidason, H., Hajdas, I., Hatte, C., Heaton, T. J., Hoffmann, D. L., Hogg, A. G., Huguen, K.
40 A., Kaiser, K. F., Kromer, B., Manning, S. W., Niu, M., Reimer, R. W., Richards, D. A.,
41 Scott, E. M., Southon, J. R., Staff, R. A., Turney, C. S. M., and van der Plicht, J.: IntCal13
42 and Marine13 radiocarbon age calibration curves 0-50,000 years cal BP, Radiocarbon, 55,
43 1869-1887, 2013.

- 1 Rogers, S. R., Fischer, M., and Huss, M.: Combining glaciological and archaeological
2 methods for gauging glacial archaeological potential, *Journal of Archaeological Science*, 52,
3 410-420, 2014.
- 4 Ruff, M., Fahrni, S., Gäggeler, H. W., Hajdas, I., Suter, M., Synal, H.-A., Szidat, S., and
5 Wacker, L.: On-line radiocarbon measurements of small samples using elemental analyzer
6 and MICADAS gas ion source, *Radiocarbon*, 52, 1645-1656, 2010.
- 7 Saloranto, T. M.: Simulating snow maps for Norway: description and statistical evaluation of
8 the seNorge snow model, *The Cryosphere*, 6, 1323-1337, 2012.
- 9 Sato, A., Takahashi, S., Naruse, R., and Wakahama, G.: Ablation and Heat Balance of the
10 Yukikabe Snow Patch in the Daisetsu Mountains, Hokkaido, Japan, *Annals of Glaciology*, 5,
11 122-126, 1984.
- 12 Sigl, M., Jenk, T. M., Kellerhals, T., Szidat, S., Gaggeler, H. W., Wachter, L., Synal, H.-A.,
13 Boutron, C., Barbante, C., Gabrieli, J., and Schwikowski, M.: Towards radiocarbon dating of
14 ice cores, *Journal of Glaciology*, 55, 985-996, 2009.
- 15 Sollid, J. L., Holmlund, P., Isaksen, K., and Harris, C.: Deep permafrost boreholes in western
16 Svalbard, northern Sweden and southern Norway, *Norwegian Journal of Geography* 54, 186–
17 191, 2000.
- 18 Spindler, K.: *The Man in the Ice: The Preserved Body of a Neolithic Man Reveals the Secrets*
19 *of the Stone Age*, Sutton, Stroud, 1994.
- 20 Suter, P. J., Hafner, A., and Glauser, K.: *Lenk – Schnidejoch. Funde aus dem Eis – ein vor-*
21 *und frühgeschichtliche Passübergang.*, *Archäologie im Kanton Bern*, 6B, 499-516, 2005.
- 22 Sørđal, I.: *Kartlegging av temperaturtilhøva i Gråsubreen og Juvfonne.*, Master, Department
23 of Geosciences, University of Oslo, Oslo, 81 pp.+ app. pp., 2013.
- 24 Tachon, M.: *Thermal regimes and horizontal surface velocities on Hellstugubreen and*
25 *Storbreen, Jotunheimen, Southern Norway*, Master, Department of Geosciences, University of
26 Oslo, Oslo, 99 pp. + app. pp., 2015.
- 27 Uglietti, C., Zapf, A., Jenk, T. M., Szidat, S., Salazar, G., and Schwikowski, M.: Radiocarbon
28 dating of glacier ice, *The Cryosphere Discuss.*, 2016. 19 pp., 2016.
- 29 UNESCO: *Perennial ice and snow masses – a guide for compilation and assemblage of data*
30 *for the World Glacier Inventory*, *Technical Papers in Hydrology*, 1, 1970.
- 31 Vedeler, M. and Jørgensen, L. B.: Out of the Norwegian glaciers: Lendbreen—a tunic from
32 the early first millennium AD, *Antiquity*, 87, 788-801, 2013.
- 33 Westermann, S., Schuler, T. V., Gislås, K., and Etzelmüller, B.: Transient thermal modeling
34 of permafrost conditions in Southern Norway, *The Cryosphere*, 7, 719-739, 2013.
- 35 Winsvold, S. H., Andreassen, L. M., and Kienholz, C.: Glacier area and length changes in
36 Norway from repeat inventories, *The Cryosphere*, 8, 1885-1903, 2014.
- 37 Zapf, A., Nesje, A., Szidat, S., Wacker, L., and Schwikowski, M.: ^{14}C measurements of ice
38 samples from the Juvfonne ice tunnel, Jotunheimen, Southern Norway—validation of a ^{14}C
39 dating technique for glacier ice, *Radiocarbon* 55, 571-578, 2013.
- 40 Zhang, Y. L., Perron, N., Ciobanu, V. G., Zotter, P., Minguillón, M. C., Wacker, L., Prévôt,
41 A. S. H., Baltensperger, U., and Szidat, S.: On the isolation of OC and EC and the optimal

- 1 strategy of radiocarbon-based source apportionment of carbonaceous aerosols, *Atmos. Chem.*
2 *Phys.*, 12, 10841-10856, 2012.
- 3 Ødegård, R.: Ground and glacier thermal regimes related to periglacial and glacial processes:
4 Case studies from Svalbard and southern Norway, 2 Dr.Scient., Dr. scient. thesis (in English),
5 Department of Geography, Rapportserie i naturgeografi, University of Oslo, Norway., Oslo,
6 44 pp. pp., 1993.
- 7 Ødegård, R., Nesje, A., Isaken, K., and Eiken, T.: Perennial ice patch studies – preliminary
8 results from a case study in Jotunheimen, southern Norway, *Geophysical Research Abstracts*
9 Vol. 13, EGU2011-12027, Vienna2011, 1.
- 10

1 Table 1.

2 Areal extents of Juvfonne derived from topographic maps, Landsat imagery, GNSS
3 measurements by foot and digitising from orthohotos. *Seasonal snow remaining along the
4 extent.

5

Year	Date	Source	Area (km ²)
1981		map	0.171
1984	10.08.1984	Orthophoto	0.208
1997	15.08.1997	Landsat	0.208
2003	09.08.2013	Landsat	0.150
2004	12.08.2004	map	0.187
2010	25.08.2010	GNSS	0.149
2011	02.08.2011	GNSS	0.150
2011	17.09.2011	Orthophoto	0.127
2012	12.09.2012	GNSS	0.160
2013	12.08.2013	GNSS	0.151
2014	09.09.2014	GNSS	0.101
2015	11.09.2015	GNSS	0.186*

6

7

1 Table 2.

2 AMS radiocarbon dates from the ice tunnels (clear ice samples and organic remains) and ice

3 samples from the ice patch surface. Ice samples collected as blocks and subdivided in several

4 sub-samples. Therefore an average value is shown for every block (JUV1, JUV2 and JUV3)

5 except for JUV0 because JUV0_1 and JUV0_2 were taken adjacent to the plant fragment

6 layer, dated 6600 cal BP (Poz-56955), while samples from JUV0_3 to JUV0_8 were collected

7 at the bottom of the wall, a few cm below the plant fragment layer. Thus JUV0_A is the

8 yielded average of JUV0_1 and JUV0_2 while the other six samples were averaged as

9 JUV0_B. Calibrated ages (cal BP) denote the 1 σ range.

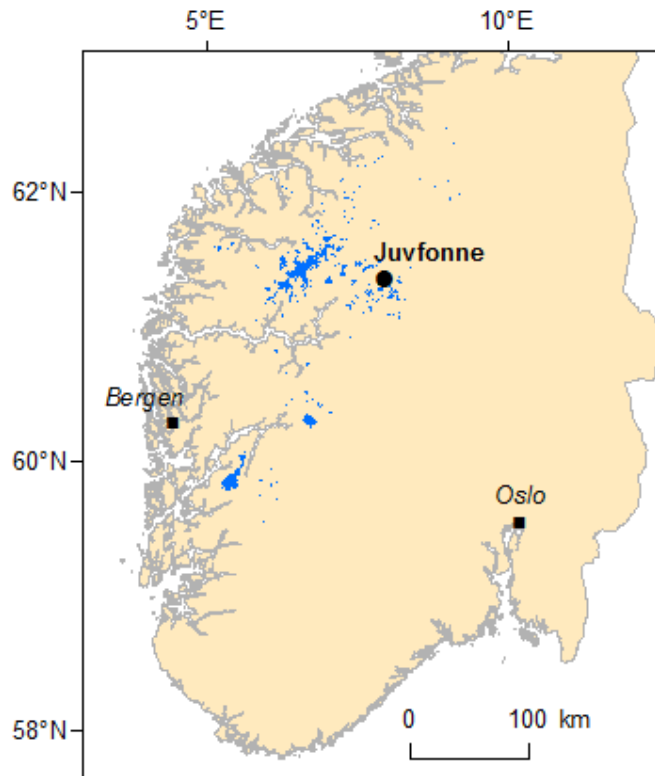
10

Sample ID	AMS Lab. No.	Type of material	^{14}C age (BP)	cal age (cal BP)	median probability (cal BP)
JUV3_1 (tunnel 2010)	ETH 42845.1.1	Surface ice	-939 ± 93		
JUV3_2 (tunnel 2010)	ETH 42847.1.1	Surface ice	-722 ± 110		
JUV3_3 (tunnel 2010)	ETH 42849.1.1	Surface ice	-1158 ± 104		
JUV3_4 (tunnel 2010)	ETH 43446.1.1	Surface ice	-1220 ± 117		
JUV3 (tunnel 2010)		Surface ice	-1010 ± 120	(-46 - -7)	-43
JUV2_1 (tunnel 2010)	ETH 43443.1.1	Ice	1018 ± 210		
JUV2_2 (tunnel 2010)	ETH 43445.1.1	Ice	1873 ± 669		
JUV2_3 (tunnel 2010)	ETH 43559.1.1	Ice	1119 ± 323		
JUV2_4 (tunnel 2010)	ETH 45109.1.1	Ice	1128 ± 287		
JUV2 (tunnel 2010)		Ice	1277 ± 207	965 - 1368	1190
Poz-37877 (tunnel 2010)	Poz-37877	Organic remains	1095 ± 30	963 - 1052	1001
Poz-37879 (tunnel 2010)	Poz-37879	Organic remains	1420 ± 30	1300 - 1338	1322
Poz-39788 (tunnel 2010)	Poz-39788	Reindeer dung	1480 ± 30	1335 - 1395	1363
Poz-37878 (tunnel 2010)	Poz-37878	Organic remains	1535 ± 30	1380 - 1518	1438
Poz-56952 (tunnel 2012)	Poz-56952	Organic remains	2025 ± 30	1929 - 2002	1974
JUV1_3 (tunnel 2010)	ETH 43555.1.1	Ice	2141 ± 304		
JUV1_4 (tunnel 2010)	ETH 43557.1.1	Ice	2650 ± 715		
JUV1 (tunnel 2010)		Ice	2386 ± 314	2011 - 2783	2450
Poz-36460(tunnel 2010)	Poz-36460	Organic remains	2960 ± 30	3074 - 3168	3121
Poz-56953 (tunnel 2012)	Poz-56953	Organic remains	3490 ± 35	3716 - 3828	3764
Poz-56954 (tunnel 2012)	Poz-56954	Organic remains	4595 ± 35	5148 - 5445	5316
Tra-4427 (tunnel 2012)	Tra-4427	Organic remains	5044 ± 100	5664 - 5904	5791
Poz-56955 (tunnel 2012)	Poz-56955	Organic remains	5800 ± 40	6555 - 6660	6600
JUV0_1 (tunnel 2010)	BE 4184.1.1	Ice	5913 ± 252		

JUV0_2 (tunnel 2010)	BE 4380.1.1	Ice	6290 ± 141		
JUV0_A (tunnel 2012)		Ice	6099 ± 240	6720 - 7256	6970
JUV0_3 (tunnel 2012)	BE 4185.1.1	Ice	6504 ± 217		
JUV0_4 (tunnel 2012)	BE 4381.1.1	Ice	6559 ± 127		
JUV0_5 (tunnel 2012)	BE 4186.1.1	Ice	7301 ± 239		
JUV0_6 (tunnel 2012)	BE 4382.1.1	Ice	6632 ± 202		
JUV0_7 (tunnel 2012)	BE 4187.1.1	Ice	7281 ± 219		
JUV0_8 (tunnel 2012)	BE 4383.1.1	Ice	6397 ± 232		
JUV0_B (tunnel 2012)		Ice	6761 ± 168	7476 - 7785	7632

1
2
3

1
2

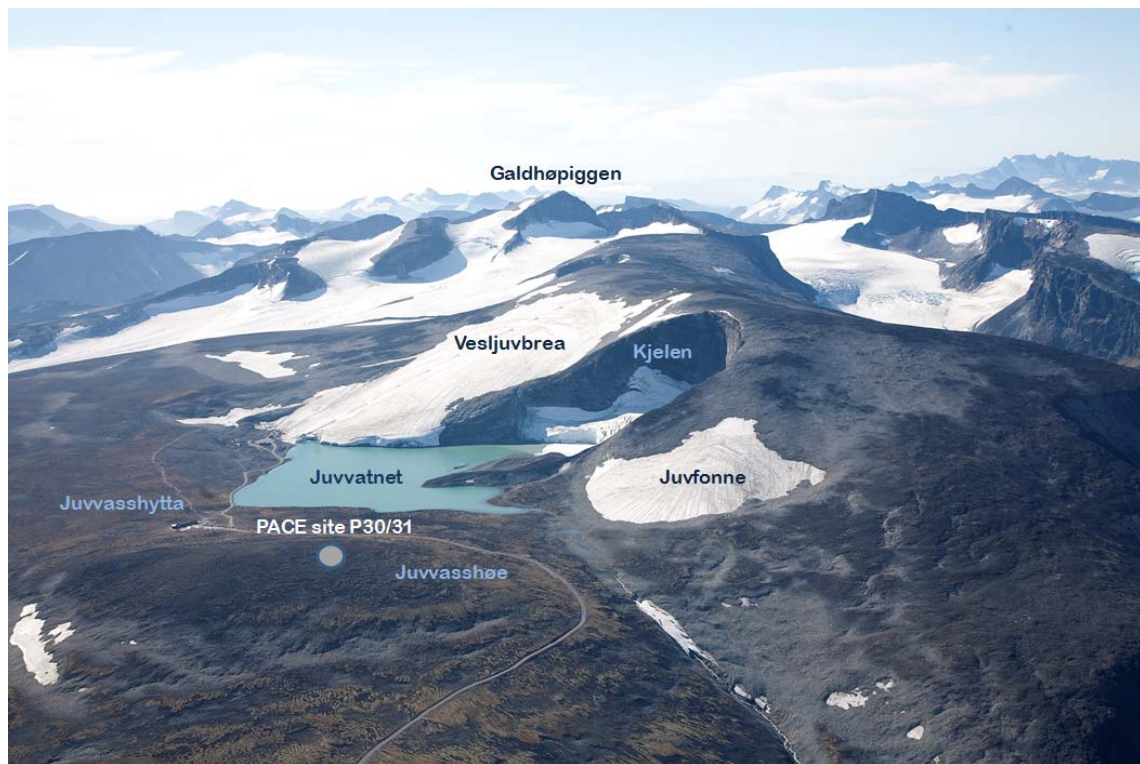


3

4

5 Figure 1. The field site Juvfonne in central southern Norway. Dark blue areas are glaciers.

6



1

2 Figure 2. Overview picture from September 2008 towards SSW showing Juvfonne and the
3 Juvflye area including Kjelen, Juvvatnet, Juvvasshytta, Vesljuvbrea and the P30/31
4 Permafrost and Climate in Europe (PACE) boreholes at Juvvasshøe. Also visible is the
5 highest mountain of Norway, Galdhøpiggen (2469 m a.s.l.). Photo: Helge J. Standal.

6

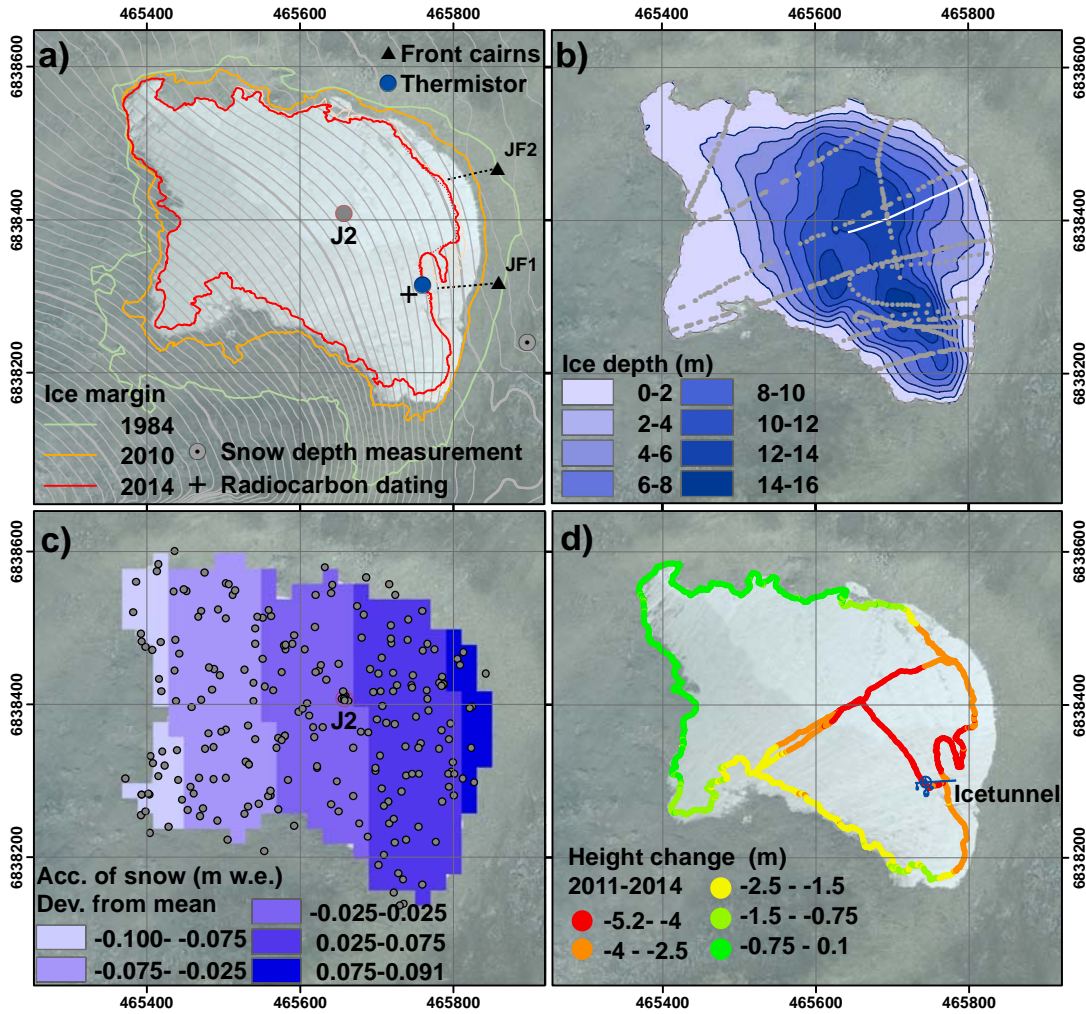
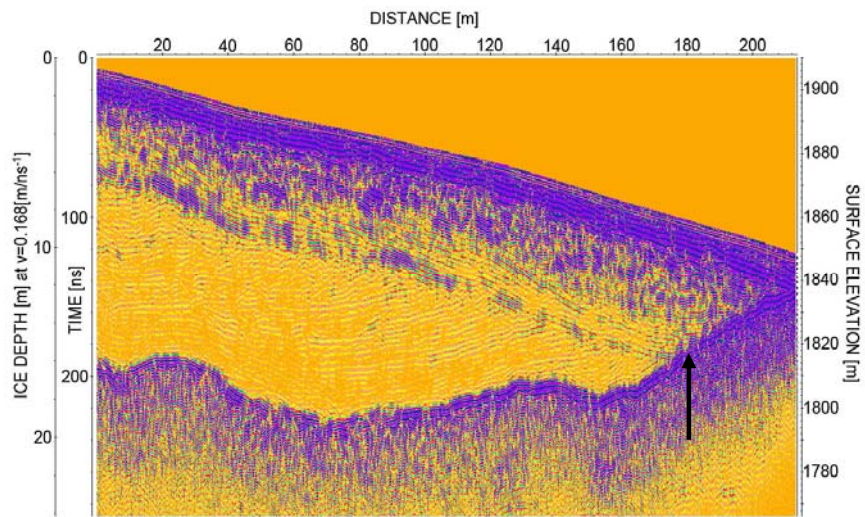


Figure 3. Maps of Juvfonne with orthophoto from September 2011 as background (UTM coordinates zone 32N), a) ice margins, position of front measurements (JF1 and JF2- see Fig. 9), position of mass balance stake J2, position of thermistor for ice temperature measurements (Fig. 13) and position of the oldest radiocarbon dating and position of snow depth measurement station, b) interpolated contours of bed topography relative to ice thickness in September 2011 (grey markers are radar points used in the interpolation) and position of the georadar track in Fig. 4 - white line, c) grey markers are snow depth measurements (2010-2015), the raster map shows a first order polynomial fit to the deviation from mean accumulation each year d) height differences along GNSS tracks in 2014 relative to ice surface from laserdata in 2011 and positions of ice tunnel excavated in 2012.



1

2 Figure 4. Example of 250 MHz Georadar profile. The position of the track shown in Fig. 3b.

3 The arrow shows the approximate minimum front position in September 2014.

4



1

2

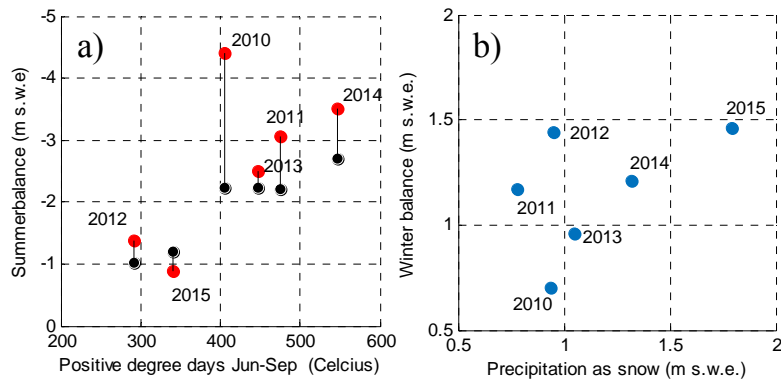
3 Figure 5. Photo of angular discontinuity at the wall of the 2010 ice tunnel, as also observed on
4 the georadar data (Fig. 4). The upper layering is parallel to the surface of Juvfonne.
5 Radiocarbon dating of the upper part showed modern age. Width of picture is approximately
6 0.4 m.

7



Figure 6. Photos of Juvfonne 17 September 2014 (a) and 10 September 2014 (b) showing the pre LIA surface exposed in central and southern parts of the ice patch (left side). The area on Juvfonne in the north-west (right side) is interpreted to be ice of modern age. The entrance of the ice tunnel is sitting on a small ridge that might be ice cored (left side lower image). The collapsed 2010 tunnel is to the left of the entrance. Photo: Glacier Archaeology Program/Oppland County Council (upper) and L. M. Andreassen (lower).

1



2

3 Figure 7. Summer (a) and winter (b) balance plotted against summer temperature (positive
 4 degree-days) and estimated precipitation as snow, respectively. For the summer balance, the
 5 black markers are calculated melt using a degree-day model with typical values calibrated
 6 from nearby glaciers (3.5 mm/°Cday for snow and 7.5 mm/°Cday for ice). Winter
 7 precipitation is obtained from seNorge (Engeset et al., 2004).

8

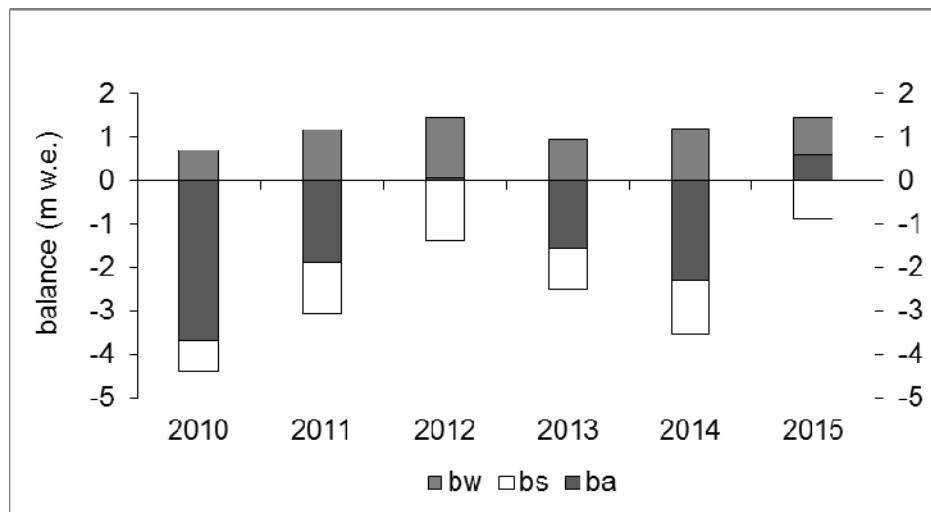


Figure 8. Mass balance measurements at stake J2 on Juvfonne: bw – balance winter, bs – balance summer, ba – annual (net) balance (Fig. 3a for position of stake).



1

2

3 Figure 9. Front position of Juvfonne measured at two locations relative to the 2010-front.

4 Minima are observed in 2011 and 2014. The front retreat 2009-2014 was measured to 69 m.

5 For position of measurements, see Fig. 3a. Red - JF1, Green – JF2.

6

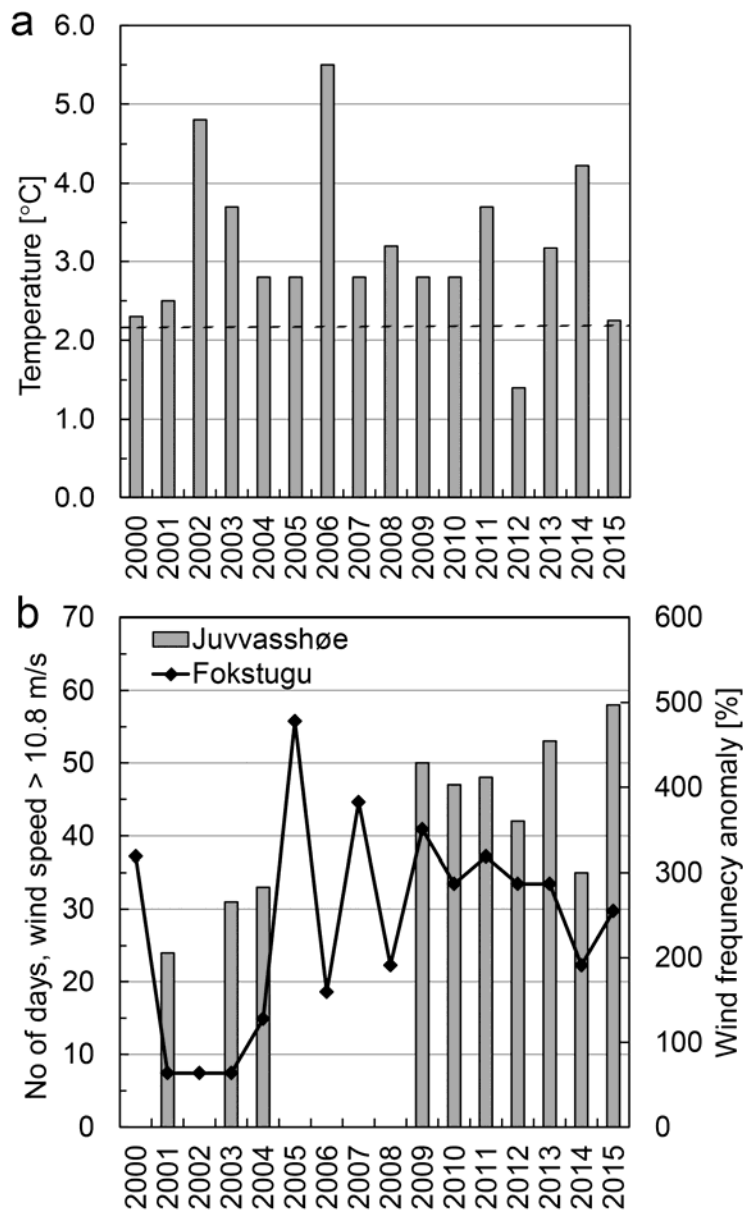


Figure 10. Meteorological data from the station at Juvvasshøe (750 m from the front of Juvfonne) and Fokstugu 70 km NE a) Juvvasshøe June-September mean Air Temperature. The black dotted line denotes the 1971-2000 mean, obtained from the interpolated seNorge dataset (Engeset et al. 2004). b) Number of days for the period June-September with strong breeze or higher (wind speed above 10.8 ms⁻¹) at Juvvasshøe (grey bars) and at Fokstugu (black line), the latter shown as anomaly (in %, right axes) with respect to 1971-2000 mean.

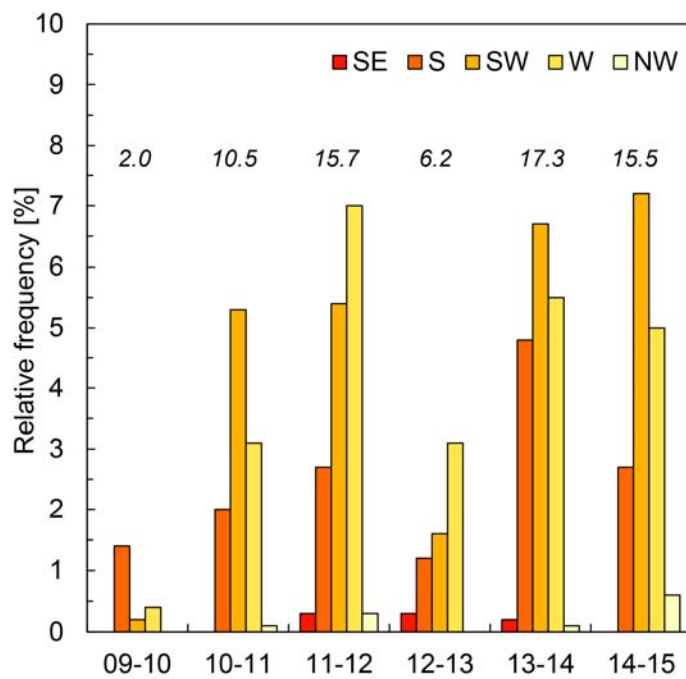


Figure 11. Relative frequency (as percentage of all hourly observations) of strong gale or more ($\geq 20.8 \text{ ms}^{-1}$) at Juvvasshøe during winter (Oct-Apr) 2009-2015 for the wind sectors SE to NW. The values inserted show the total frequency of strong gale or more.

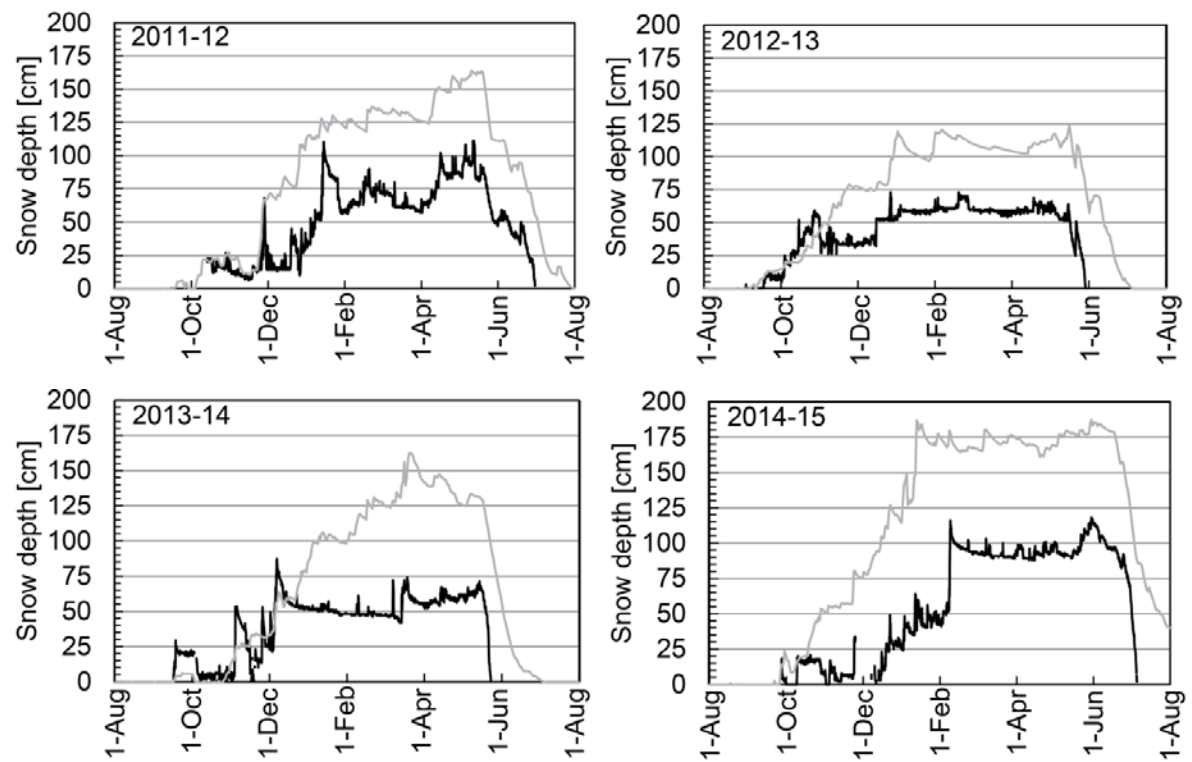
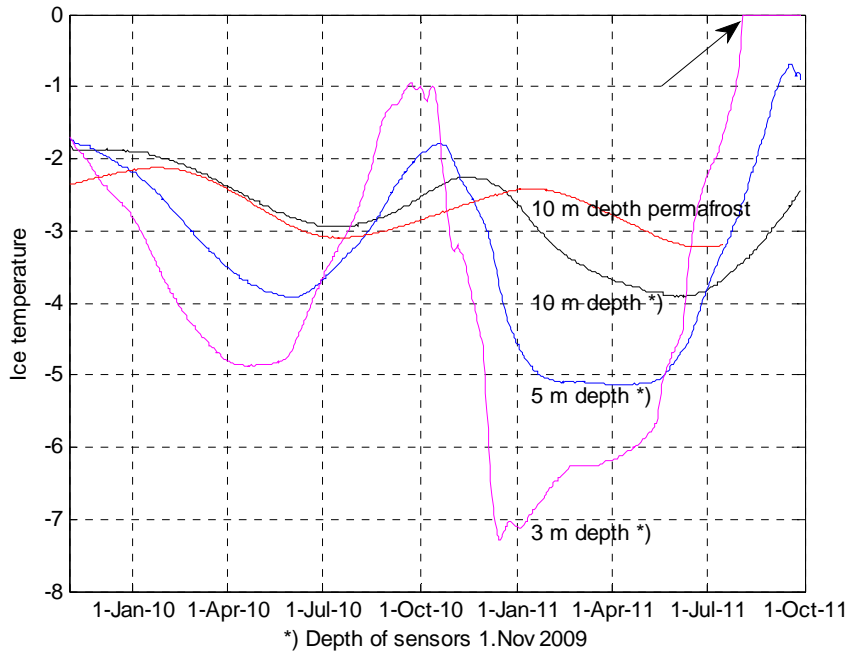


Figure 12. Hourly snow depth measurements (black lines) from the station 95 m from the front of Juvfonne (see Figure 3a for position). Grey lines show modelled daily snow depth from seNorge (Engeset et al. 2004).

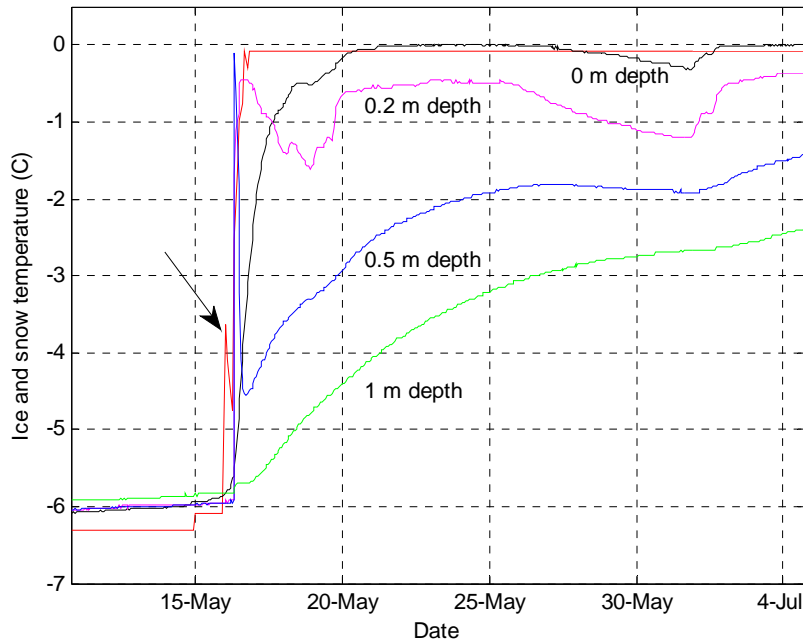


1

2

3 Figure 13. Temperature for November 2009-September 2011 in a 10 m deep borehole in the
 4 Juvfonne ice patch (see Fig. 3a for position). The red line is the temperature at 10 m depth in
 5 the P31 permafrost borehole 750 m north from the ice patch (see Fig. 2 for location). Arrow
 6 points to the time when the sensor placed at 3 m depth in autumn 2009 melted out. The entire
 7 thermistor string melted out in mid-September 2014.

8

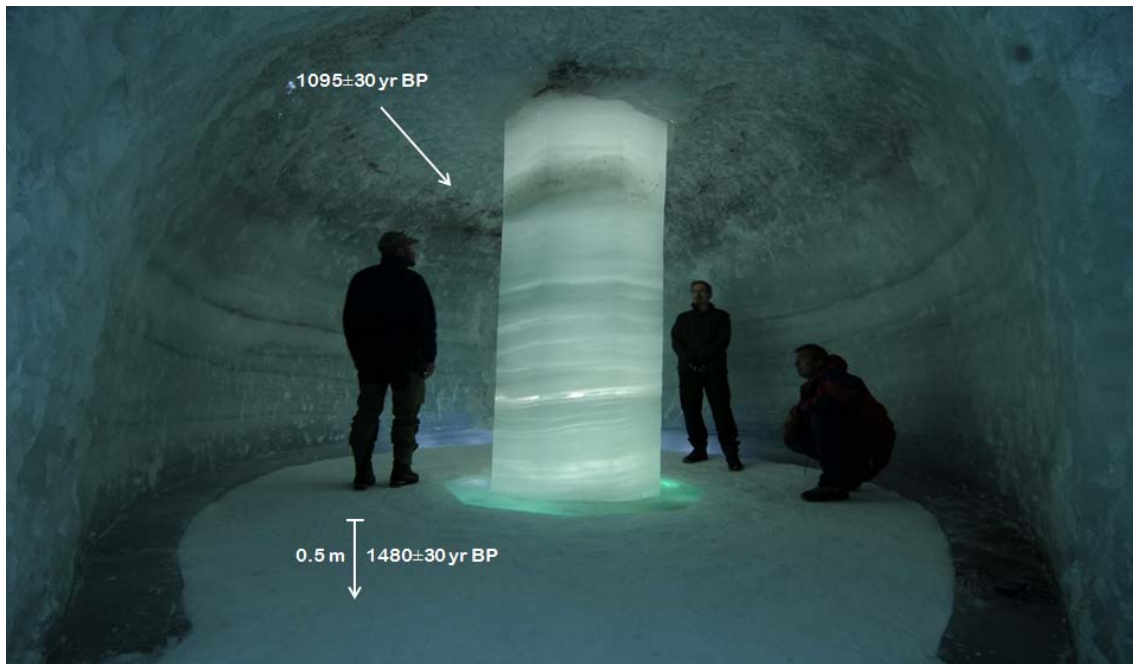


1

2

3 Figure 14. Plot of temperature measurements in ice and snow at the onset of thaw in May
 4 2010 (position at the thermistor shown in Fig. 3a). The depth reference is the ice surface the
 5 previous autumn. The red line is the snow temperature 0.25 m from the base of the snow
 6 cover. The arrow point the first signal of surface meltwater refreezing close to the base of the
 7 snow cover.

8

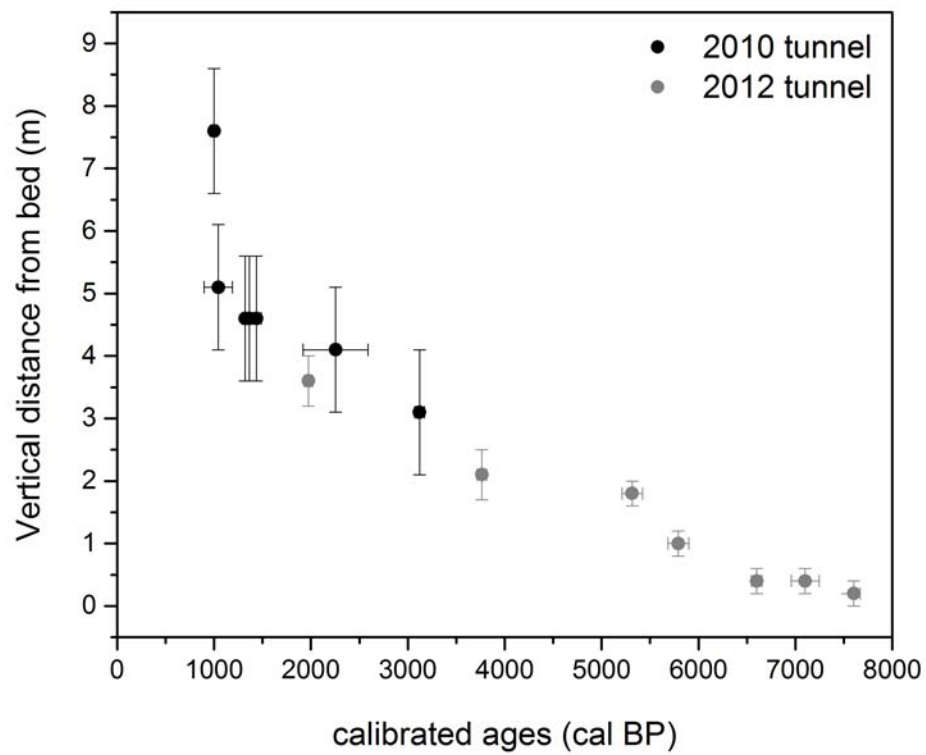


1

2

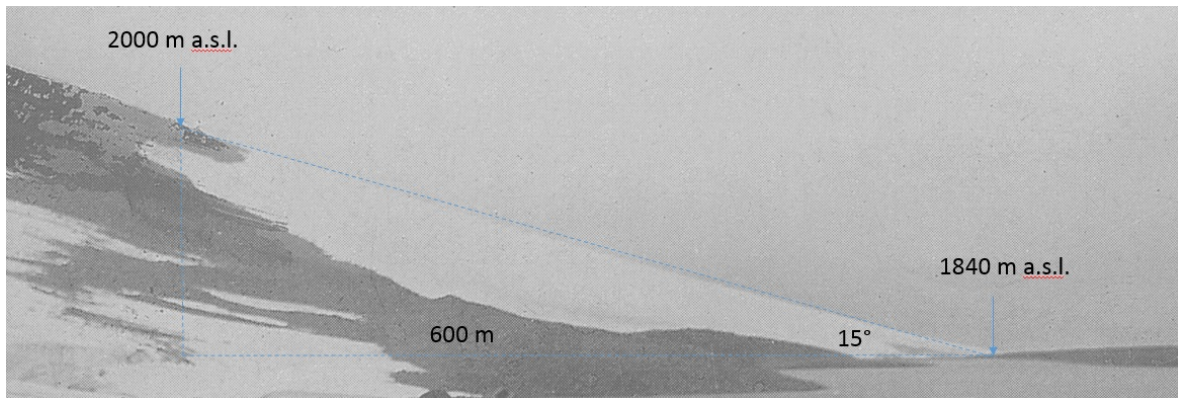
3 Figure 15. Photo from the old ice tunnel excavated in 2010 showing the layering in the ice
4 and position of two samples for radiocarbon dating. Photo: Klimapark2469 AS.

5



1
2 Figure 16. Plot of the samples in Table 2 except samples with modern age. In the inner parts
3 of the 2012 tunnel the bed is partly exposed, which gives good distance to bed estimates. In
4 the 2010 tunnel, the distance estimates depend on the radar data (the old tunnel partly melted
5 out). The horizontal distance between the samples are up to 50 m.

6



1

2 Figure 17. Picture taken from Vesljuvbrea towards NNW showing Juvfonne from around
3 1900. The surface slope of Juvfonne is approximately 15°. Height and length estimate from
4 map based on position in the picture. The upper and northern part of Juvfonne cannot be seen
5 on the picture.

6

7